Post-transcriptional gene regulation by the RNA binding protein IGF2BP3 is critical for MLL-AF4 mediated leukemogenesis

Tiffany M Tran[1,2], Julia Philipp[3], Jaspal Bassi[1], Neha Nibber[1], Jolene Draper[3], Tasha Lin[4,5], Jayanth Kumar Palanichamy[1,6], Amit Kumar Jaiswal[1], Oscar Silva[7], May Paing[1], Jennifer King[8], Sol Katzman[3], Jeremy R. Sanford[3], Dinesh S. Rao[1,2,9,10,11*]

[1] Department of Pathology and Laboratory Medicine, David Geffen School of Medicine at UCLA, Los Angeles, California, USA.
[2] Molecular, Cellular and Integrative Physiology Graduate Program, UCLA, Los Angeles, California, 90095, USA.
[3]Department of Molecular, Cellular and Developmental Biology, UCSC, Santa Cruz, California, 95064, USA.
[4]Division of Hematology/Oncology, Department of Medicine at UCLA, Los Angeles, California, 90095, USA.
[5] Molecular Biology Graduate Program, UCLA, Los Angeles, California, 90095, USA.
[6]Department of Biochemistry, All India Institute of Medical Sciences, New Delhi, 110029, India
[7]Department of Pathology, Stanford University School of Medicine, Stanford, California, 94305, USA.
[8]Division of Rheumatology, Department of Medicine at UCLA, Los Angeles, California, 90095, USA.
[9]Jonsson Comprehensive Cancer Center (JCCC) and
[10]Broad Stem Cell Research Center, UCLA, Los Angeles, California, 90095, USA.
[11]Lead Contact
*Correspondence: DRao@mednet.ucla.edu

Conflict of interest statement: The authors declare no competing interests.

ABSTRACT

Despite recent advances in therapeutic approaches, patients with MLL-rearranged leukemia still have poor outcomes and a high risk of relapse. Here, we found that MLL-AF4, the most common MLL fusion protein in patients, transcriptionally induces IGF2BP3 and that IGF2BP3 strongly amplifies MLL-Af4 mediated leukemogenesis. Deletion of *Igf2bp3* significantly increases the survival of mice with MLL-Af4 driven leukemia and greatly attenuates disease. At the cellular level, MLL-Af4 leukemia-initiating cells require *Igf2bp3* for their function in leukemogenesis. eCLIP and transcriptome analysis of MLL-Af4 transformed stem and progenitor cells and MLL-Af4 bulk leukemia cells reveals a complex IGF2BP3-regulated post-transcriptional operon governing leukemia cell survival and proliferation. Critical mRNA targets include important leukemogenic genes such as in the *Hoxa* locus and numerous genes within the Ras signaling pathway. Together, our findings show that IGF2BP3 is an essential positive regulator of MLL-AF4 mediated leukemogenesis and is a potential therapeutic target in this disease.

INTRODUCTION

Chromosomal rearrangements of the mixed-lineage leukemia (*MLL*, also known as *KMT2A*) gene are recurrently found in a subset of acute lymphoblastic leukemia (ALL), acute myeloid leukemia (AML), and in acute leukemia of ambiguous lineage (1). Despite recent advances in therapeutic approaches, patients with *MLL*-rearranged (MLLr) leukemia have very poor outcomes, a high risk of relapse, and show resistance to novel targeted therapies (2, 3) (4-6). *MLL* encodes a H3K4 methyltransferase that has been shown to be required for hematopoietic stem cell (HSC) development during both embryonic and adult hematopoiesis (7, 8). Many of the translocation partners for *MLL*, including *AF4 (AFF1),* encode proteins that regulate transcriptional elongation (9-11). Of more than 90 translocation fusion partner genes, *MLL-AF4* (*KMT2A-AFF1*) is the most common *MLL* fusion protein in patients (12). Biologically, *MLL-AF4*-driven leukemia is a distinct entity, with a unique gene expression profile showing significant overlap with stem cell programs (13, 14).

At the post-transcriptional level, emerging evidence suggests a role for microRNAs, RNA-binding proteins, and other novel mechanisms in regulating gene expression during leukemogenesis (15-19). We recently identified the oncofetal RNA binding protein (RBP) Insulin like growth factor 2 mRNA binding protein 3 (IGF2BP3) as an important regulator of gene expression in *MLL*-rearranged B-ALL (15). IGF2BP3 is expressed during embryogenesis, lowly expressed in healthy adult tissues, and strongly re-expressed in cancer cells (20, 21). Several studies have shown that elevated levels of IGF2BP3 expression are correlated with diminished patient survival in many cancer types and may be a marker of disease aggressiveness in B-ALL (22-25). Previously, we determined that overexpression of IGF2BP3 in the bone marrow (BM) of mice leads to a pathologic expansion of hematopoietic stem and progenitor cells (HSPC), in a manner dependent on RNA binding. IGF2BP3 interacts primarily with the 3'UTR of its target transcripts, as with MYC and CDK6, resulting in an upregulation of transcript and protein (15). In the case of MYC and CDK6, IGF2BP3 binding resulted in upregulation of target transcript and

protein, with attendant effects on pathologic hematopoietic stem and progenitor cell expansion. Together, these studies illuminated a novel role for post-transcriptional gene regulation in the pathologic proliferation of HSPCs.

Experimentally, MLL-AF4 driven leukemogenesis has been studied using a range of *in vitro* and *in vivo* models leading to significant progress in our understanding of MLL-rearranged leukemia (13, 26-30). Here, we explicitly tested the requirement for *Igf2bp3* in a bona-fide *in vivo* model of MLL-Af4 driven leukemogenesis (31). Deletion of *Igf2bp3* significantly increased the survival of MLL-Af4 transplanted mice and decreased the numbers and self-renewal capacity of MLL-Af4 leukemia-initiating cells (LICs). Mechanistically, we found that IGF2BP3 targets and modulates the expression of transcripts within the *Hoxa* locus and components of the Ras signaling pathway, both key regulators of leukemogenesis, through multiple post-transcriptional mechanisms (32, 33). Together, our findings show that IGF2BP3 is a critical regulator of MLL-AF4 mediated leukemogenesis and a potential therapeutic target in this disease (32, 33).

RESULTS

The MLL-AF4 fusion protein transcriptionally induces IGF2BP3

To determine the functional impact of IGF2BP3 expression on MLL-AF4-mediated gene expression, we compared IGF2BP3-regulated targets with a published dataset of MLL-Af4 targets obtained by ChIP-Seq (15, 31). Transcripts modulated by IGF2BP3 were significantly enriched for MLL-Af4-bound genes (Figure 1A; Supplemental Figure 1A). Next, to test if *IGF2BP3* was a direct transcriptional target of MLL-AF4, we performed ChIP-PCR assays on RS4;11 and SEM cell lines, human B-ALL cell lines that contain the MLL-AF4 translocation, and determined that a region in the first intron of *IGF2BP3* is strongly bound by MLL-AF4 (Figure 1B; Supplemental Figure 1B) (34). This MLL-AF4 binding was abrogated when SEM cells were treated with the bromodomain inhibitor, iBET-151 (Figure 1C)(35). Furthermore, we observed an MLL-AF4-dose-dependent increase in luciferase reporter activity, using a 950bp promoter region upstream of the transcription start site (TSS) of IGF2BP3 (Supplemental Figure 1C). To confirm that MLL-AF4 not only binds to the *IGF2BP3* gene but also promotes its expression, we utilized a retroviral MSCV vector encoding the human *MLL* fused to the murine *Af4* (MLL-Af4)(31). In the murine pre-B cell line, 70Z/3, and primary murine bone marrow cells, we found that MLL-Af4 transduction caused an approximately 64-fold upregulation of *Igf2bp3* mRNA (Figure 1D-E). Concordantly, IGF2BP3 protein was upregulated in MLL-Af4 transduced primary bone marrow cells, after being undetectable in control cells (Figure 1F). Taken together, these findings demonstrate that MLL-Af4 drives the expression of *Igf2bp3 in vivo*.

Normal hematopoiesis is maintained in Igf2bp3 KO mice

To test the *in vivo* requirement for IGF2BP3 in leukemogenesis, we generated an *Igf2bp3* KO (I3KO) mouse. We initially generated a floxed *Igf2bp3* allele (f/f; Supplemental Figure 2A) using CRISPR/Cas9. In the course of mating the mice with the Vav1-Cre mouse strain, we serendipitously generated a germline knockout allele (del), which we isolated and further characterized (Supplemental Figure 2B). Mendelian inheritance was confirmed, although

the distribution of genotypes was marginally skewed (Table S1). Deletion of *Igf2bp3* was confirmed at the DNA, RNA, and protein level (Supplemental Figure 2C-E). Thus, *Igf2bp3*$^{del/del}$ (I3KO) mice were used for the remainder of the study. Immunophenotyping of I3KO mice showed no significant differences in the numbers of HSPCs in the BM compared to WT (Supplemental Figure 2F). Additionally, I3KO mice showed similar numbers of myeloid-lineage progenitors (including CMPs, GMPs, and MEPs)(Supplemental Figure 2G) and normal B-cell development as assessed by the Hardy scheme (36) (Supplemental Figure 2H) and normal numbers of mature B-lymphoid, T-lymphoid, and myeloid lineages in the BM and spleen (Supplemental Figure 2I-J). Hence, I3KO mice demonstrate preserved normal, steady-state adult hematopoiesis, although specific differences in other hematopoiesis conditions need further investigation.

Igf2bp3 deletion increases the latency of MLL-Af4 leukemia and survival of mice

After confirmation of preserved baseline hematopoiesis in I3KO mice, we next utilized bone marrow transplantation (BMT) assays to query MLL-Af4 mediated leukemogenesis (Supplemental Figure 3A). Retroviral MLL-Af4 transduction was equivalent between WT and I3KO donor BM, based on DNA copy number analysis (Supplemental Figure 3B) and Western blot analysis for MLL-Af4 (Supplemental Figure 3C). Following transplantation of the transduced HSPCs, we found that the loss of *Igf2bp3* significantly increases both the leukemia-free and overall survival of MLL-Af4 mice (Figure 2A-B). The median survival of WT/MLL-Af4 mice was 103 days while I3KO/MLL-Af4 mice had a median survival of greater than 157 days. Complete blood counts of WT/MLL-Af4 mice showed a consistent increase in WBC and absolute myeloid counts over time, which was severely blunted in I3KO/MLL-Af4 mice (Figure 2C; Supplemental Figure 3D). On average, peripheral blood counts crossed the leukemic threshold much earlier in WT/MLL-Af4 mice compared to I3KO/MLL-Af4 mice (70 days versus 112 days) (Figure 2C). Concordantly, peripheral blood smears showed reduced circulating blasts in I3KO/MLL-Af4 mice

versus WT/MLL-Af4 mice (Supplemental Figure 3E). Together, these findings indicated that *Igf2bp3* is required for efficient MLL-Af4-mediated leukemogenesis.

Igf2bp3 modulates disease severity in MLL-Af4-driven leukemia

The MLL-Af4 model utilized here causes a highly penetrant, aggressive form of leukemia in mice. To characterize the role of *Igf2bp3* in disease severity, we performed detailed immunophenotypic and histopathologic analyses in MLL-Af4-transplanted mice in timed experiments. I3KO/MLL-Af4 transplanted mice showed a highly significant approximately 4-fold reduction in spleen weights at 14 weeks post-transplant compared to WT/MLL-Af4 transplanted mice (Figure 2D). We observed near-total infiltration of the spleen and liver by leukemic cells, obliterating the normal tissue architecture in WT/MLL-Af4 mice, a finding that was much reduced in I3KO/MLL-Af4 mice (Figure 2E). In line with this, I3KO/MLL-Af4 transplanted mice showed a significant reduction in CD11b+ cells (Figure 2G; Supplemental Figure 3G), which were less proliferative (CD11b+Ki-67+), both in the spleen (approximately 30-fold) and in the BM (approximately 2.5-fold) at 14 weeks (Figure 2F; Supplemental Figure 3F). Thus, *Igf2bp3* deletion significantly reduces the tumor burden and attenuates disease severity in MLL-Af4 transplanted mice.

Igf2bp3 is required for LIC function in vitro

Several studies highlight the importance of LICs in both human and mouse leukemia. In the MLL-Af4 model, these LICs show expression of CD11b and c-Kit (14, 37, 38). Given our findings of delayed initiation and decreased disease severity, we characterized these LICs, and found that I3KO/MLL-Af4 transplanted mice showed a significant 10-fold decrease in the numbers of leukemia-initiating cells (CD11b+c-Kit+) in the spleen and a 5-fold decrease in the BM at 14 weeks compared to WT/MLL-Af4 mice (Figure 3A-B). To further characterize the MLL-Af4 LIC and its dependence on IGF2BP3, we turned to endpoint colony formation assays. Utilizing immortalized HSPCs, denoted as Lin-, from WT/MLL-Af4 and I3KO/MLL-Af4 mice, we confirmed of equal transcript expression levels of MLL-Af4 and deletion of IGF2BP3 at the

protein level (Figure 3C; Supplemental Figure 5A-B). The deletion of *Igf2bp3* resulted in an approximately 2-fold reduction in total colony formation as well as a significant decrease in CFU-GM progenitors (Figure 3D). To confirm our findings regarding LICs, we utilized an orthogonal method to delete *Igf2bp3* via CRISPR-Cas9. Briefly, Lin- cells from Cas9-GFP BL/6 mice were collected and transduced with the retroviral MSCV-MLL-Af4 vector. After selection, these MLL-Af4 Cas9-GFP Lin- cells were transduced with a retroviral vector with an mCherry fluorescence marker containing either a non-targeting (NT) sgRNA or a sgRNA targeted against *Igf2bp3* (I3sg) (Figure 3E). Importantly, *Igf2bp3* is deleted after transformation with MLL-Af4, a distinction from the previous method. After confirmation of *Igf2bp3* deletion (Figure 3F-G), GFP+mCherry+ MLL-Af4 Lin- cells were utilized for colony-forming assays. We confirmed that CRISPR-Cas9 mediated deletion of *Igf2bp3* led to a significant reduction in total colony numbers and decreases in the various colony morphologies (Figure 3H). The observed differences in overall colony forming capacity between the two systems are most likely a result of the different methodologies being used, but in both systems, IGF2P3 deficiency led to decreased colony formation. Thus, *Igf2bp3* is required for MLL-Af4 LIC function *in vitro*.

Igf2bp3 is necessary for the function of _MLL-Af4_ leukemia-initiating cells _in vivo_

Since *Igf2bp3* deletion causes a reduction in LICs and is required for the function of these LICs, we next wanted to determine if *Igf2bp3* specifically affects the capability of these LICs to initiate MLL-Af4 leukemia *in vivo*. First, to investigate baseline hematopoietic stem cell function in I3KO mice, we completed a competitive repopulation bone marrow transplantation experiment by transplanting lethally irradiated CD45.1 recipient mice with 50% of either WT or I3KO CD45.2 donor BM and 50% CD45.1 donor BM. We found no defect in engraftment over time in transplant recipients of I3KO BM (Supplemental Figure 4A). Moreover, we determined no differences in multilineage hematopoietic reconstitution ability of I3KO donor cells, as immature lineages in the BM and mature B-hematopoietic cells in the periphery were intact (Supplemental Figure 4B-H, respectively). Given that there were no baseline differences in

reconstitution by normal HSPCs, we now sought to determine if *Igf2bp3* impacted the number of effective LICs in secondary transplant assays. We isolated BM cells from WT/MLL-Af4 and I3KO/MLL-Af4 mice with equivalent disease burdens and transplanted equal numbers (10^6, 10^5, and 10^4) of leukemic BM cells into immunocompetent CD45.1 mice. At 4 weeks post-transplantation, mice that received 10^6 cells from I3KO/MLL-Af4 mice had significantly reduced donor CD45.2+ cell engraftment (Figure 4A). With 10^5 and 10^4 transplanted cells, we no longer observed measurable leukemic burden in recipient mice (Figure 4A). This suggests that the active cell frequency of LICs in I3KO/MLL-Af4 mice is lost between 10^6 and 10^5 cells (Figure 4A)(39). Moreover, WBC and splenic weights were significantly decreased in I3KO/MLL-Af4 leukemia transplanted mice (Figure 4B-D). Histologically, leukemic infiltration was absent in the spleen and liver of 10^5 transplanted I3KO/MLL-Af4 mice (Figure 4E). Thus, *Igf2bp3* deletion greatly attenuated transplantability, in which only 17% of I3KO/MLL-Af4 recipients developed leukemia while 67% of WT/MLL-Af4 recipients developed leukemia at 4 weeks with 10^6 transplanted cells (Figure 4B). These data show that the deletion of *Igf2bp3* results in the significant reduction of LICs and reconstitution of MLL-Af4 transplanted mice, suggesting that *Igf2bp3* is necessary for the self-renewal capability of LICs *in vivo*.

IGF2BP3 supports oncogenic gene expression networks in LIC-enriched and bulk leukemia cells

To determine how IGF2BP3 amplifies the MLL-Af4 gene expression, we performed eCLIP to identify IGF2BP3 bound transcripts in both Lin- and CD11b+ cells. Sequencing libraries were prepared from a minimum of two biological replicates with two technical replicates (four immunoprecipitations per cell line) as well as size matched input (smInput) samples from each condition. After filtering out reads that overlap the smInput, reproducible peaks were identified by using CLIPper (40). Although the majority of peaks were present within introns, we observed cell type-specific differences in the locations of IGF2BP3 binding sites within exons. In CD11b+ cells, a greater proportion of exonic peaks were found in 3'UTRs whereas a greater

proportion of peaks mapped to internal exons in Lin- cells (Figure 5A-B). To identify differentially expressed transcripts related to the I3KO phenotype, we sequenced RNA from WT/MLL-Af4 and I3KO/MLL-Af4 Lin- and CD11b+ bulk leukemia cells (Figure 5C-D, respectively). First, we confirmed expression of MLL and *Igf2bp3* in these samples by RT-qPCR and WB (Figure 3C; Supplemental Figure 5A-E). DEseq2 revealed hundreds of differentially expressed transcripts (Figure 5C-D; Tables S2 and S3) (41). We observed 208 upregulated and 418 downregulated transcripts in the CD11b+ cells, and 189 upregulated and 172 downregulated transcripts in the Lin- cells. A significant fraction of these differentially expressed mRNAs are bound by IGF2BP3 ($P< 2.2x10^{-}16$; Supplemental Figure 6A). Motif analysis revealed an enrichment of CA-rich elements as expected (Supplemental Figure 6B) (42). To identify over-represented pathways and gene ontology terms within IGF2BP3 differentially regulated transcripts, we used the Metascape analysis tool (43) and observed a significant enrichment in transcripts associated with the KEGG pathway related to transcriptional misregulation in cancer in both the Lin- and CD11b+ bulk leukemia dataset (Figure 5E-F). Interestingly, there were also distinct oncogenic networks that were regulated in the two datasets, with regulation of signaling pathways noted in the Lin- cells (PI3K/AKT) and in the CD11b+ cells (GTPase, MAPK pathway) (Figure 5E-F). This was also confirmed by an independent analysis of differentially expressed data using GSEA, where we noted that the Hallmark KRAS pathway was significantly enriched in the CD11b+ cells (Supplemental Figure 5G). Furthermore, we observed a significant enrichment for GO oxidative phosphorylation in the Lin- cells (Supplemental 5H). We used RT-qPCR to validate the RNA-seq data from both Lin- and CD11b+ cells. In Lin- cells, we focused on differentially regulated genes with a known leukemogenic function including *Csf2rb, Notch1*, *Cd69,* and the *Hoxa* cluster of transcripts, including *Hoxa9*, *Hoxa10, Hoxa7*. We observed a significant decrease in the steady state mRNA levels for each of these transcripts in the I3KO/MLL-Af4 Lin- cells, confirming the RNA sequencing results (Figure 5G). To confirm our findings in CD11b+ cells, we selected target transcripts known to play a role in Ras signaling,

Ccnd1, *Maf*, *Mafb Itga6, Klf4, and Akt3* (44-50). As expected, these transcripts were decreased in I3KO/MLL-Af4 CD11b+ cells, confirming the high throughput RNA sequencing findings (Figure 5H). Furthermore, we determined that there was a significant decrease in Ras GTPase activity in the I3KO/MLL-Af4 CD11b+ cells compared to WT/MLL-Af4 CD11b+ bulk leukemia cells using a commercial ELISA assay (Supplemental Figure 5I). Together, this data demonstrates that IGF2BP3 plays a major role in amplifying the expression of many cancer-related genes in Lin- and CD11b+ cells.

IGF2BP3 regulates alternative pre-mRNA splicing

A recent study indicated that IGF2BP3 may regulate alternative pre-mRNA splicing (51). The eCLIP data revealed numerous peaks within precursor mRNA (pre-mRNA) in both Lin- and CD11b+ cells, suggesting a potential role in splicing regulation. To test this hypothesis, we utilized MISO (Mixture of Isoforms) analysis to identify differentially spliced transcripts in WT/MLL-Af4 and I3KO/MLL-Af4 cells (52). Across both cell lines, we identified hundreds of transcripts with IGF2BP3-dependent changes in alternative splicing, including 97 differential splicing events in the Lin- and 261 splicing events in the CD11b+ cells (Supplemental Figure 6C). Most event types, including skipped exons (SE), alternative first exons (AFE), alternative last exons (ALE), alternative 3' splice sites (A3SS), and alternative 5' splice sites (A5SS) exhibited both increases and decreases in PSI, however, intron retention (RI) events showed a consistent reduction in splicing in the I3KO/MLL-Af4 cells (Figure 6A). A significant fraction of alternatively spliced transcripts contained IGF2BP3 binding sites in proximity of the splicing event ($P<2.2x10^{-16}$, Supplementary Figure 6D). After merging all replicate eCLIP data for each cell type, we determined the position of eCLIP peaks relative to splice sites for splicing events identified by MISO (Figure 6B). Across all event types we found that the density of IGF2BP3 binding sites was strongest near the 3'splice site (3'ss), with additional signal near the 5' splice site (5'ss). This pattern was observed for each distinct splicing event class that MISO identified, with retained introns exhibiting the strongest bias towards the 3'ss (Supplemental Figure 6E).

This positional bias in the data was noted for some differentially expressed genes, such as *Hoxa9*, *Hoxa7*, and *Cd69* (Figure 6C; Supplemental 6F). *Hoxa9* is known to be alternatively spliced, with two well-characterized transcripts, full-length *Hoxa9* and truncated (homeobox-less) *Hoxa9T* (53, 54). We designed and validated RT-qPCR primers to measure the two RNA isoforms, finding that I3KO/MLL-Af4 cells showed an alteration in the ratio of the two isoforms (Figure 6D). This was in addition to our previous finding that the total transcript (using primers that are isoform-agnostic) was also downregulated in I3KO/MLL-Af4 cells (Figure 5G). Hence, the net effect of IGF2BP3 may be multi-pronged—there is a strong impact on steady state mRNA levels, and there is potentially an impact on splicing. Taken together, these data demonstrate that IGF2BP3 functions in regulation of alternative pre-mRNA splicing in bulk leukemia cells and progenitor cells.

DISCUSSION

Here, we have generated an *Igf2bp3*–deficient murine model and queried MLL-Af4 mediated leukemogenesis. We demonstrated that *Igf2bp3* is required for the efficient initiation of leukemia and that this regulates the number and frequency of MLL-Af4 LICs. *Igf2bp3* regulates the expression of numerous critical transcripts in the *Hoxa* locus and the Ras signaling pathway, leading to dysregulated gene expression and enhanced downstream signaling, thereby promoting leukemogenesis.

MLL-AF4 driven leukemogenesis is associated with massive transcriptional dysregulation, mediated by the fusion of a histone methyltransferase with a factor involved in the super elongation complex (9). We demonstrate here for the first time that *Igf2bp3* is a direct transcriptional target of the MLL-AF4 fusion protein. Interestingly, IGF2BP3 itself seems to positively regulate MLL-AF4 transcriptional targets, based on our analysis provided here. Together, these data suggest that IGF2BP3 forms a novel post-transcriptional feed-forward loop that stabilizes and/or enhances the expression of MLL-Af4 transcriptional targets.

In our previous study, we determined that IGF2BP3 is required for B-ALL cell survival, and that overexpression of IGF2BP3 in the bone marrow of mice leads to a pathologic expansion of hematopoietic stem and progenitor cells (15). Here, using the MLL-Af4 leukemia model, we found that the deletion of *Igf2bp3* caused a striking delay in leukemia development and significantly increased the survival of MLL-Af4 mice. Furthermore, *Igf2bp3* deficiency greatly attenuated the aggressiveness of the disease. This was demonstrated by significant decreases in WBC counts, spleen weights, and infiltrating leukemic cells visualized in histopathological analysis of hematopoietic tissues. Although MLL-Af4 drives an acute myeloid leukemia in mice (31), it is important to note that *MLL*r leukemias often show lineage infidelity and plasticity, leading to difficulties in applying targeted therapy (5). While our prior work focused on IGF2BP3 in B-lineage *MLL*r leukemia, the current work suggests its broader applicability to all *MLL*r leukemia. Hence, IGF2BP3 may be a constant factor to target across

the phenotypic range of *MLL*r leukemia and may be less subject to change in response to targeted therapy.

We also determined that *Igf2bp3* regulates the numbers and function of leukemia-initiating cells (LICs). Importantly, the effect of *Igf2bp3* deletion was restricted to LICs and did not significantly impact normal HSC function. Deletion of *Igf2bp3* led to a LIC disadvantage *in vivo* and *in vitro*, using both the I3KO mouse and a novel, orthogonal system utilizing CRISPR/Cas9-mediated deletion of *Igf2bp3*. LICs have been defined as cells that can self-renew and have the capability to produce downstream bulk leukemia cells (55). The persistence of these LICs is thought to contribute to relapse after treatment in several different leukemia subtypes (56-59). In *MLL*r leukemia, LICs have been shown to have a high frequency in tumors and co-expression of mature lineage-restricted cell markers, with some excellent work in mouse models (14, 38, 60). However, the details of human LICs, particularly in MLL-AF4 leukemia, are less well known (27, 61-63). The role of IGF2BP3 in such cells will be of great interest and is a future direction for our work.

Previously, we discovered that IGF2BP3 interacts primarily with the 3'UTR of its target transcripts via iCLIP-seq (15). In this study, we determined that IGF2BP3 targets many transcripts within intronic regions and near splice sites in addition to the 3'UTR, suggesting additional roles in post-transcriptional gene regulation. This difference may be due to the use of the eCLIP technique or the focused application on primary cells as opposed to cell lines. It is not entirely surprising, however, since RBPs are known to regulate gene expression at several steps at the post-transcriptional level through mRNA operons (64, 65). Furthermore, a recent study has shown that IGF2BP3 may regulate alternative splicing in the PKM gene in lung cancer cells (51). In line with this study, we also found dynamic alternative splicing events that belonged to Retained Introns, Alternative 5' Splice Sites, Alternative 3' Splice Sites, and Skipped Exons. Thus, IGF2BP3 likely regulates specific mRNA operons through multiple post-transcriptional mechanisms in the MLL-Af4 leukemia context.

Notably, we observed that these differentially regulated transcripts showed significant enrichment for the KEGG pathway of transcriptional misregulation in cancer through Metascape as well as GO oxidative phosphorylation through GSEA. Notable IGF2BP3 targets included critical transcripts in the *Hoxa* cluster such as *Hoxa9, Hoxa10, and Hoxa7.* HOXA9 is induced by MLL-AF4, plays a role in normal hematopoiesis, and is required for the survival of MLL-rearranged leukemia (66-71). Furthermore, Hoxa9 is an alternatively spliced gene, with co-expression of a homeodomain-less splice variant, *Hoxa9T*, together with *Hoxa9*, shown to be necessary for full leukemogenic transformation (53, 54). Hence, *Igf2bp3* may act through upregulation of *Hoxa9* and *Hoxa9T* through multiple post-transcriptional mechanisms to promote MLL-Af4 driven leukemogenesis and impact the function of MLL-Af4 LICs. In addition, HOXA9 may play a role in the regulation of oxidative phosphorylation (72), and it is tempting to speculate that the observed *Igf2bp3*-dependent impact on LICs is a consequence of dysregulated oxidative phosphorylation, a key pathway that regulates LICs. Importantly, because *Igf2bp3* was not required for steady-state hematopoiesis, in contrast to HOXA9, it may represent a more attractive target.

Work from our lab and others have demonstrated that IGF2BP3 targets a wide array of oncogenic transcripts and pathways, including CDK6 and MYC (73). Here, we found that IGF2BP3 targets and modulates the expression of many transcripts within the Ras signaling pathway and its downstream effector pathways. Thus, IGF2BP3 likely regulates activation of the PI3K/Akt/mTOR, Rho/Rac, Ralgds/RalA, and the MAPK/ERK pathways in MLL-Af4 bulk leukemia cells. RAS proteins control numerous cellular processes such as proliferation and survival, and are amongst the most commonly mutated genes in cancer (32, 74). Interestingly, while *MLL*r leukemias have a paucity of additional mutations, the most common mutations are in the RAS signaling pathway (61, 75-81). Moreover, several studies have shown selective activity against MLL-r leukemia cell lines and primary samples *in vitro* by MEK inhibitors, suggesting the potential role of signaling downstream of RAS mutations in leukemia survival(78, 79, 82).

Here, we determined that *Igf2bp3* is required for the efficient initiation of MLL-Af4 driven leukemia as well as for the development of and self-renewal capability of MLL-Af4 LICs. Mechanistically, IGF2BP3 binds to hundreds of transcripts and modulates their expression *in vivo* and *in vitro* through multiple, complex post-transcriptional mechanisms. We describe a novel positional bias for IGF2BP3 binding in leukemic cells isolated from an *in vivo* model, a notable advance. In summary, our study demonstrated that IGF2BP3 is an amplifier of *MLL*r leukemogenesis by targeting *Hoxa* transcripts essential for leukemia-initiating cell function and targeting Ras signaling pathway transcripts, thereby controlling multiple critical downstream effector pathways required for disease initiation and severity. Our findings highlight IGF2BP3 as a necessary regulator of MLLr leukemia and a potential therapeutic target for this disease.

METHODS

ChIP-PCR. RS4;11 and SEM cells were used for ChIP assays as previously described (83). Primer sequences for the IGF2BP3 promoter region were provided by James Mulloy (University of Cincinnati College of Medicine)(31).

Western Blotting and RT-qPCR. Protein and mRNA extracts were prepared, and Western Blot/RT-qPCR performed as previously described (73, 84). Primers for qPCR and antibodies used for Western blotting are listed in Table S4.

Plasmids. The MSCV-MLL-flag-*Af4* plasmid was kindly provided by Michael Thirman (University of Chicago, Department of Medicine) through MTA (31). The non-targeting or *Igf2bp3* sgRNA was cloned into an in-house MSCV-hU6-sgRNA-EFS-mCherry vector.

Retroviral transduction and bone marrow transplantation. Retroviral transduction and bone marrow transplantation (BMT) were completed as previously described (73, 84-86). 5-FU enriched BM and Lin- cells were spin-infected four times with MSCV-MLL-flag-*Af4* virus at 30°C for 45 minutes in the presence of polybrene. Cells were selected with 400 µg/ml of G418 for 7 days. For sgRNA-mediated knockout, MLL-Af4 overexpressing Cas9-GFP cells were retrovirally infected with MSCV-hU6-NT/I3sgRNA-EFS-mCherry. The selected cells were then cultured for colony formation assays or injected into lethally irradiated mice.

Mice. C57BL/6J and B6J.129(Cg)-Gt(ROSA)26Sor$^{tm1.1(CAG-cas9*,-EGFP)Fezh}$/J (Cas9-GFP) mice were obtained from Jackson Laboratory. For *Igf2bp3* KO mouse generation, the UCI Transgenic Mouse Facility utilized CRISPR/Cas9 to insert loxP sites flanking exon 2 of *Igf2bp3* to generate *Igf2bp3*$^{f/f}$ mice. We originally attempted to generate conditional KO mice by breeding the *Igf2bp3*$^{f/f}$ mice with Vav1-Cre mice. Consistent with prior reports, we found that this strategy led to “leaky” Cre expression, resulting in germline deletion (87-91). To isolate the floxed and

deletion (del) alleles, we back-crossed the mice onto C57BL/6 mice, successfully confirming germline, Mendelian transmission of the del and floxed alleles in two successive generations (Table S1). Mice heterozygous for the del allele were mated together, with the production of a homozygous deletion of *Igf2bp3*, resulting in the *Igf2bp3*$^{del/del}$ mice (I3KO) used in this study.

Cell culture. RS4;11, SEM, 70Z/3 and HEK 293T cell lines were cultured as previously described (73, 84). Lin- cells were cultured in IMDM with 15% fetal bovine serum supplemented with SCF, IL-6, FLT3, and TPO. CD11b+ cells were isolated from splenic tumors for positive selection by CD11b antibody and MACS (Miltenyi).

Flow cytometry. Blood, BM, thymus, and spleen were collected from the mice under sterile conditions at the indicated time points and staining performed as previously described (73, 84, 92). The list of antibodies used is provided in Table S4. Flow cytometry was performed on a BD FACS LSRII. Analysis was performed using FlowJo software.

Histopathology. Fixation and sectioning has been described previously (85). Analysis was performed by a board certified hematopathologist (D.S. Rao).

Competitive repopulation assay and secondary leukemia transplantation. Competitive repopulation experiments were completed as previously described (73). For leukemia transplantation, BM was collected from WT/MLL-Af4 or I3KO/MLL-Af4 mice that succumbed to leukemia at 10-14 weeks post-transplantation and injected into 8-week-old immunocompetent CD45.1+ female mice.

eCLIP. IGF2BP3 crosslinking-immunoprecipitation studies were carried out in triplicate in each cell type using Eclipse BioInnovations eCLIP kit. Briefly, $5x10^5$ cells were crosslinked with

245nm UV radiation at 400mJoules/cm^2. Crosslinked cell lysates were treated with RNAse I to fragment RNA and immunoprecipitated with anti-IGF2BP3 antibody (MBL RN009P) coupled to magnetic Protein G beads. Paired-end RNA sequencing was performed on the Illumina HiSeq4000 system at the UCSF Genomics Core Facility. Peaks were called using CLIPper (40). Annotation of the genomic location of the peaks and motif enrichment analysis were performed using HOMER (93) annotatePeaks.pl and findMotifs.pl, respectively. Background for the peaks within differentially expressed genes was simulated using bedtools (93, 94) and shuffled 1000 times.

RNA seq. Single-end, strand-specific RNA sequencing was performed on the Illumina HiSeq3000 system for the Lin- and CD11b+ samples, resulting in 15-20 million reads per sample, at the UCLA Technology Center for Genomics & Bioinformatics. Our analysis pipeline has been previously described (73). Enrichment analysis for KEGG pathways and Gene Ontology (GO) biological processes terms was completed with the Metascape analysis tool (http://metascape.org)(43). Gene Set Enrichment Analysis (GSEA) was completed using the GSEAPreranked software on both the Lin- and CD11b+ DESeq datasets after calculation of π-value (95-97) to compare to the Hallmark and GO gene sets within the Molecular Signatures Database.

Statistics. Data represent mean ±SD for continuous numerical data, unless otherwise noted in the figure legends. One-way ANOVA followed by Bonferroni's multiple comparisons test or 2-tailed Student's t tests were performed using GraphPad Prism software. One-way ANOVA followed by Bonferroni's multiple comparisons test was performed in experiments with more than two groups.

Data Sharing Statement. Raw and analyzed data have been deposited onto the NCBI Gene Expression Omnibus (GEO) repository (GSE156115).

AUTHOR CONTRIBUTIONS

T.M.T., J.B., N.N., J.P., J.D., T.L., J.K.P., A.K.J., M.P., and J.K. performed experiments. T.M.T., J.P., and S.K. analyzed results and made the figures. O.S. provided experimental resource. T.M.T. and D.S.R. designed the research and wrote the paper. T.M.T., J.B., N.N., J.P., T.L., J.K.P., O.S., J.K., J.R.S., D.S.R. reviewed and edited the paper.

ACKNOWLEDGEMENTS

This work was supported by the Tumor Cell Biology Training Grant NIH T32 CA009056 (T.M.T.), NIH/NIGMS R35GM130361 (J.R.S.), NIH/NCI R01CA166540 (D.S.R.), NIH/NCI R21CA197441 (D.S.R.), American Society of Hematology Bridge Grant (D.S.R.), UCLA Jonsson Comprehensive Cancer Center Seed Grant (D.S.R.) and STOPCancer/Barbara and Gary Luboff Mitzvah Fund Seed Grant (D.S.R.). Flow cytometry was performed in the Eli and Edythe Broad Center of Regenerative Medicine and Stem Cell Research UCLA Flow Cytometry Core Resource and the UCLA JCCC/CFAR Flow Cytometry Core Facility that is supported by NIH AI-28697, P30CA016042, the JCCC, the UCLA AIDS Institute, and the David Geffen School of Medicine at UCLA. The authors acknowledge the support of the Chao Family Comprehensive Cancer Center Transgenic Mouse Facility (TMF) Shared Resource, supported by the National Cancer Institute of the National Institutes of Health under award number P30CA062203. The content is solely the responsibility of the authors and does not necessarily represent the official views of the National Institutes of Health. The authors would like to thank Jon Neumann (TMF), Michael O. Alberti, and Jorge Contreras for their expertise and helpful discussions.

REFERENCES

1. Krivtsov AV, and Armstrong SA. MLL translocations, histone modifications and leukaemia stem-cell development. *Nature Reviews Cancer.* 2007;7(11):823-33.
2. Moorman AV, Ensor HM, Richards SM, Chilton L, Schwab C, Kinsey SE, et al. Prognostic effect of chromosomal abnormalities in childhood B-cell precursor acute lymphoblastic leukaemia: results from the UK Medical Research Council ALL97/99 randomised trial. *The Lancet Oncology.* 2010;11(5):429-38.
3. Pui C-H, Carroll WL, Meshinchi S, and Arceci RJ. Biology, Risk Stratification, and Therapy of Pediatric Acute Leukemias: An Update. *Journal of Clinical Oncology.* 2011;29(5):551-65.
4. Haddox CL, Mangaonkar AA, Chen D, Shi M, He R, Oliveira JL, et al. Blinatumomab-induced lineage switch of B-ALL with t(4:11)(q21;q23) KMT2A/AFF1 into an aggressive AML: pre- and post-switch phenotypic, cytogenetic and molecular analysis. *Blood Cancer Journal.* 2017;7(9):e607-e.
5. Rayes A, McMasters RL, and O'Brien MM. Lineage Switch in MLL-Rearranged Infant Leukemia Following CD19-Directed Therapy. *Pediatr Blood Cancer.* 2016;63(6):1113-5.
6. Wei J, Wunderlich M, Fox C, Alvarez S, Cigudosa JC, Wilhelm JS, et al. Microenvironment Determines Lineage Fate in a Human Model of MLL-AF9 Leukemia. *Cancer Cell.* 2008;13(6):483-95.
7. Ernst P, Fisher JK, Avery W, Wade S, Foy D, and Korsmeyer SJ. Definitive Hematopoiesis Requires the Mixed-Lineage Leukemia Gene. *Developmental Cell.* 2004;6(3):437-43.
8. Jude CD, Climer L, Xu D, Artinger E, Fisher JK, and Ernst P. Unique and Independent Roles for MLL in Adult Hematopoietic Stem Cells and Progenitors. *Cell Stem Cell.* 2007;1(3):324-37.
9. Smith E, Lin C, and Shilatifard A. The super elongation complex (SEC) and MLL in development and disease. *Genes & Development.* 2011;25(7):661-72.
10. Lin C, Smith ER, Takahashi H, Lai KC, Martin-Brown S, Florens L, et al. AFF4, a Component of the ELL/P-TEFb Elongation Complex and a Shared Subunit of MLL Chimeras, Can Link Transcription Elongation to Leukemia. *Molecular Cell.* 2010;37(3):429-37.
11. Mohan M, Lin C, Guest E, and Shilatifard A. Licensed to elongate: a molecular mechanism for MLL-based leukaemogenesis. *Nature Reviews Cancer.* 2010;10(10):721-8.
12. Meyer C, Burmeister T, Gröger D, Tsaur G, Fechina L, Renneville A, et al. The MLL recombinome of acute leukemias in 2017. *Leukemia.* 2018;32(2):273-84.
13. Krivtsov AV, Feng Z, Lemieux ME, Faber J, Vempati S, Sinha AU, et al. H3K79 Methylation Profiles Define Murine and Human MLL-AF4 Leukemias. *Cancer Cell.* 2008;14(5):355-68.
14. Somervaille TCP, Matheny CJ, Spencer GJ, Iwasaki M, Rinn JL, Witten DM, et al. Hierarchical maintenance of MLL myeloid leukemia stem cells employs a transcriptional program shared with embryonic rather than adult stem cells. *Cell stem cell.* 2009;4(2):129-40.
15. Palanichamy JK, Tran TM, Howard JM, Contreras JR, Fernando TR, Sterne-Weiler T, et al. RNA-binding protein IGF2BP3 targeting of oncogenic transcripts

promotes hematopoietic progenitor proliferation. *J Clin Invest.* 2016;126(4):1495-511.

16. Ennajdaoui H, Howard Jonathan M, Sterne-Weiler T, Jahanbani F, Coyne Doyle J, Uren Philip J, et al. IGF2BP3 Modulates the Interaction of Invasion-Associated Transcripts with RISC. *Cell Reports.* 2016;15(9):1876-83.
17. Park S-M, Gönen M, Vu L, Minuesa G, Tivnan P, Barlowe TS, et al. Musashi2 sustains the mixed-lineage leukemia–driven stem cell regulatory program. *J Clin Invest.* 2015;125(3):1286-98.
18. Jønson L, Christiansen J, Hansen Thomas VO, Vikeså J, Yamamoto Y, and Nielsen Finn C. IMP3 RNP Safe Houses Prevent miRNA-Directed HMGA2 mRNA Decay in Cancer and Development. *Cell Reports.* 2014;7(2):539-51.
19. Nguyen Liem H, Robinton Daisy A, Seligson Marc T, Wu L, Li L, Rakheja D, et al. Lin28b Is Sufficient to Drive Liver Cancer and Necessary for Its Maintenance in Murine Models. *Cancer Cell.* 2014;26(2):248-61.
20. Mueller-Pillasch F, Pohl B, Wilda M, Lacher U, Beil M, Wallrapp C, et al. Expression of the highly conserved RNA binding protein KOC in embryogenesis. *Mech Dev.* 1999;88(1):95-9.
21. Mueller F, Bommer M, Lacher U, Ruhland C, Stagge V, Adler G, et al. KOC is a novel molecular indicator of malignancy. *British journal of cancer.* 2003;88(5):699-701.
22. Schaeffer DF, Owen DR, Lim HJ, Buczkowski AK, Chung SW, Scudamore CH, et al. Insulin-like growth factor 2 mRNA binding protein 3 (IGF2BP3) overexpression in pancreatic ductal adenocarcinoma correlates with poor survival. *BMC Cancer.* 2010;10:59.
23. Kobel M, Xu H, Bourne PA, Spaulding BO, Shih Ie M, Mao TL, et al. IGF2BP3 (IMP3) expression is a marker of unfavorable prognosis in ovarian carcinoma of clear cell subtype. *Mod Pathol.* 2009;22(3):469-75.
24. Lochhead P, Imamura Y, Morikawa T, Kuchiba A, Yamauchi M, Liao X, et al. Insulin-like growth factor 2 messenger RNA binding protein 3 (IGF2BP3) is a marker of unfavourable prognosis in colorectal cancer. *Eur J Cancer.* 2012;48(18):3405-13.
25. Stoskus M, Gineikiene E, Valceckiene V, Valatkaite B, Pileckyte R, and Griskevicius L. Identification of characteristic IGF2BP expression patterns in distinct B-ALL entities. *Blood Cells, Molecules, and Diseases.* 2011;46(4):321-6.
26. Chen W, Li Q, Hudson WA, Kumar A, Kirchhof N, and Kersey JH. A murine Mll-AF4 knock-in model results in lymphoid and myeloid deregulation and hematologic malignancy. *Blood.* 2006;108(2):669-77.
27. Metzler M, Forster A, Pannell R, Arends MJ, Daser A, Lobato MN, et al. A conditional model of MLL-AF4 B-cell tumourigenesis using invertor technology. *Oncogene.* 2006;25(22):3093-103.
28. Bursen A, Schwabe K, Rüster B, Henschler R, Ruthardt M, Dingermann T, et al. The AF4·MLL fusion protein is capable of inducing ALL in mice without requirement of MLL·AF4. *Blood.* 2010;115(17):3570-9.
29. Tamai H, Miyake K, Takatori M, Miyake N, Yamaguchi H, Dan K, et al. Activated K-Ras protein accelerates human MLL/AF4-induced leukemo-lymphomogenicity in a transgenic mouse model. *Leukemia.* 2011;25(5):888-91.

30. Montes R, Ayllon V, Gutierrez-Aranda I, Prat I, Hernandez-Lamas MC, Ponce L, et al. Enforced expression of MLL-AF4 fusion in cord blood CD34+ cells enhances the hematopoietic repopulating cell function and clonogenic potential but is not sufficient to initiate leukemia. *Blood.* 2011;117(18):4746-58.
31. Lin S, Luo Roger T, Ptasinska A, Kerry J, Assi Salam A, Wunderlich M, et al. Instructive Role of MLL-Fusion Proteins Revealed by a Model of t(4;11) Pro-B Acute Lymphoblastic Leukemia. *Cancer Cell.* 2016;30(5):737-49.
32. Downward J. Targeting RAS signalling pathways in cancer therapy. *Nature Reviews Cancer.* 2003;3(1):11-22.
33. Milne TA, Kim J, Wang GG, Stadler SC, Basrur V, Whitcomb SJ, et al. Multiple Interactions Recruit MLL1 and MLL1 Fusion Proteins to the HOXA9 Locus in Leukemogenesis. *Molecular Cell.* 2010;38(6):853-63.
34. Wilkinson Adam C, Ballabio E, Geng H, North P, Tapia M, Kerry J, et al. RUNX1 Is a Key Target in t(4;11) Leukemias that Contributes to Gene Activation through an AF4-MLL Complex Interaction. *Cell reports.* 2013;3(1):116-27.
35. Dawson MA, Prinjha RK, Dittmann A, Giotopoulos G, Bantscheff M, Chan W-I, et al. Inhibition of BET recruitment to chromatin as an effective treatment for MLL-fusion leukaemia. *Nature.* 2011;478(7370):529-33.
36. Hardy RR, and Hayakawa K. B Cell Development Pathways. *Annual Review of Immunology.* 2001;19(1):595-621.
37. Lin S, Luo RT, Shrestha M, Thirman MJ, and Mulloy JC. The full transforming capacity of MLL-Af4 is interlinked with lymphoid lineage commitment. *Blood.* 2017;130(7):903-7.
38. Somervaille TCP, and Cleary ML. Identification and characterization of leukemia stem cells in murine MLL-AF9 acute myeloid leukemia. *Cancer Cell.* 2006;10(4):257-68.
39. Brien CA, Kreso A, and Jamieson CHM. Cancer Stem Cells and Self-renewal. *Clinical Cancer Research.* 2010;16(12):3113.
40. Lovci MT, Ghanem D, Marr H, Arnold J, Gee S, Parra M, et al. Rbfox proteins regulate alternative mRNA splicing through evolutionarily conserved RNA bridges. *Nature structural & molecular biology.* 2013;20(12):1434-42.
41. Love MI, Huber W, and Anders S. Moderated estimation of fold change and dispersion for RNA-seq data with DESeq2. *Genome Biology.* 2014;15(12):550.
42. Schneider T, Hung L-H, Aziz M, Wilmen A, Thaum S, Wagner J, et al. Combinatorial recognition of clustered RNA elements by the multidomain RNA-binding protein IMP3. *Nature Communications.* 2019;10(1):2266.
43. Zhou Y, Zhou B, Pache L, Chang M, Khodabakhshi AH, Tanaseichuk O, et al. Metascape provides a biologist-oriented resource for the analysis of systems-level datasets. *Nature Communications.* 2019;10(1):1523.
44. Brundage ME, Tandon P, Eaves DW, Williams JP, Miller SJ, Hennigan RH, et al. MAF mediates crosstalk between Ras-MAPK and mTOR signaling in NF1. *Oncogene.* 2014;33(49):5626-36.
45. Eychène A, Rocques N, and Pouponnot C. A new MAFia in cancer. *Nature Reviews Cancer.* 2008;8(9):683-93.

46. Takata M, Goto Y, Ichii N, Yamaura M, Murata H, Koga H, et al. Constitutive Activation of the Mitogen-Activated Protein Kinase Signaling Pathway in Acral Melanomas. *Journal of Investigative Dermatology.* 2005;125(2):318-22.
47. Wagle M-C, Kirouac D, Klijn C, Liu B, Mahajan S, Junttila M, et al. A transcriptional MAPK Pathway Activity Score (MPAS) is a clinically relevant biomarker in multiple cancer types. *npj Precision Oncology.* 2018;2(1):7.
48. Wu Y, Tan X, Liu P, Yang Y, Huang Y, Liu X, et al. ITGA6 and RPSA synergistically promote pancreatic cancer invasion and metastasis via PI3K and MAPK signaling pathways. *Experimental Cell Research.* 2019;379(1):30-47.
49. Lewis A, Park CS, Puppi M, and Lacorazza HD. KLF4 Controls Leukemic Stem Cell Self-Renewal in MLL-AF9-Induced Acute Myeloid Leukemia. *Blood.* 2019;134(Supplement_1):1231-.
50. Riverso M, Montagnani V, and Stecca B. KLF4 is regulated by RAS/RAF/MEK/ERK signaling through E2F1 and promotes melanoma cell growth. *Oncogene.* 2017;36(23):3322-33.
51. Xueqing H, Jun Z, Yueqiang J, Xin L, Liya H, Yuanyuan F, et al. IGF2BP3 May Contributes to Lung Tumorigenesis by Regulating the Alternative Splicing of PKM. *Frontiers in Bioengineering and Biotechnology.* 2020;8:679.
52. Katz Y, Wang ET, Airoldi EM, and Burge CB. Analysis and design of RNA sequencing experiments for identifying isoform regulation. *Nature Methods.* 2010;7(12):1009-15.
53. He M, Chen P, Arnovitz S, Li Y, Huang H, Neilly MB, et al. Two isoforms of HOXA9 function differently but work synergistically in human MLL-rearranged leukemia. *Blood Cells Mol Dis.* 2012;49(2):102-6.
54. Stadler CR, Vegi N, Mulaw MA, Edmaier KE, Rawat VPS, Dolnik A, et al. The leukemogenicity of Hoxa9 depends on alternative splicing. *Leukemia.* 2014;28(9):1838-43.
55. Magee Jeffrey A, Piskounova E, and Morrison Sean J. Cancer Stem Cells: Impact, Heterogeneity, and Uncertainty. *Cancer Cell.* 2012;21(3):283-96.
56. Bao S, Wu Q, McLendon RE, Hao Y, Shi Q, Hjelmeland AB, et al. Glioma stem cells promote radioresistance by preferential activation of the DNA damage response. *Nature.* 2006;444(7120):756-60.
57. Chu S, McDonald T, Lin A, Chakraborty S, Huang Q, Snyder DS, et al. Persistence of leukemia stem cells in chronic myelogenous leukemia patients in prolonged remission with imatinib treatment. *Blood.* 2011;118(20):5565-72.
58. Diehn M, Cho RW, Lobo NA, Kalisky T, Dorie MJ, Kulp AN, et al. Association of reactive oxygen species levels and radioresistance in cancer stem cells. *Nature.* 2009;458(7239):780-3.
59. Merlos-Suárez A, Barriga Francisco M, Jung P, Iglesias M, Céspedes María V, Rossell D, et al. The Intestinal Stem Cell Signature Identifies Colorectal Cancer Stem Cells and Predicts Disease Relapse. *Cell Stem Cell.* 2011;8(5):511-24.
60. Krivtsov AV, Twomey D, Feng Z, Stubbs MC, Wang Y, Faber J, et al. Transformation from committed progenitor to leukaemia stem cell initiated by MLL–AF9. *Nature.* 2006;442(7104):818-22.
61. Agraz-Doblas A, Bueno C, Bashford-Rogers R, Roy A, Schneider P, Bardini M, et al. Unraveling the cellular origin and clinical prognostic markers of infant B-cell

acute lymphoblastic leukemia using genome-wide analysis. *Haematologica.* 2019;104(6):1176-88.

62. Bardini M, Woll PS, Corral L, Luc S, Wittmann L, Ma Z, et al. Clonal variegation and dynamic competition of leukemia-initiating cells in infant acute lymphoblastic leukemia with MLL rearrangement. *Leukemia.* 2015;29(1):38-50.
63. Barrett Neil A, Malouf C, Kapeni C, Bacon Wendi A, Giotopoulos G, Jacobsen Sten Eirik W, et al. Mll-AF4 Confers Enhanced Self-Renewal and Lymphoid Potential during a Restricted Window in Development. *Cell Reports.* 2016;16(4):1039-54.
64. Keene JD. RNA regulons: coordination of post-transcriptional events. *Nature Reviews Genetics.* 2007;8(7):533-43.
65. Keene JD, and Lager PJ. Post-transcriptional operons and regulons co-ordinating gene expression. *Chromosome Research.* 2005;13(3):327-37.
66. Faber J, Krivtsov AV, Stubbs MC, Wright R, Davis TN, van den Heuvel-Eibrink M, et al. HOXA9 is required for survival in human MLL-rearranged acute leukemias. *Blood.* 2009;113(11):2375-85.
67. Ernst P, Mabon M, Davidson AJ, Zon LI, and Korsmeyer SJ. An Mll-Dependent Hox Program Drives Hematopoietic Progenitor Expansion. *Current Biology.* 2004;14(22):2063-9.
68. Imamura T, Morimoto A, Takanashi M, Hibi S, Sugimoto T, Ishii E, et al. Frequent co-expression of HoxA9 and Meis1 genes in infant acute lymphoblastic leukaemia with MLL rearrangement. *British Journal of Haematology.* 2002;119(1):119-21.
69. Lawrence HJ, Christensen J, Fong S, Hu Y-L, Weissman I, Sauvageau G, et al. Loss of expression of the Hoxa-9 homeobox gene impairs the proliferation and repopulating ability of hematopoietic stem cells. *Blood.* 2005;106(12):3988-94.
70. Pineault N, Helgason CD, Lawrence HJ, and Humphries RK. Differential expression of Hox, Meis1, and Pbx1 genes in primitive cells throughout murine hematopoietic ontogeny. *Experimental Hematology.* 2002;30(1):49-57.
71. Rozovskaia T, Feinstein E, Mor O, Foa R, Blechman J, Nakamura T, et al. Upregulation of Meis1 and HoxA9 in acute lymphocytic leukemias with the t(4 : 11) abnormality. *Oncogene.* 2001;20(7):874-8.
72. Lynch JR, Salik B, Connerty P, Vick B, Leung H, Pijning A, et al. JMJD1C-mediated metabolic dysregulation contributes to HOXA9-dependent leukemogenesis. *Leukemia.* 2019;33(6):1400-10.
73. Palanichamy JK, Tran TM, Howard JM, Contreras JR, Fernando TR, Sterne-Weiler T, et al. RNA-binding protein IGF2BP3 targeting of oncogenic transcripts promotes hematopoietic progenitor proliferation. *J Clin Invest.* 2016;126(4):1495-511.
74. Schubbert S, Shannon K, and Bollag G. Hyperactive Ras in developmental disorders and cancer. *Nature Reviews Cancer.* 2007;7(4):295-308.
75. Andersson AK, Ma J, Wang J, Chen X, Gedman AL, Dang J, et al. The landscape of somatic mutations in infant MLL-rearranged acute lymphoblastic leukemias. *Nature Genetics.* 2015;47(4):330-7.

76. Chandra P, Luthra R, Zuo Z, Yao H, Ravandi F, Reddy N, et al. Acute Myeloid Leukemia With t(9;11)(p21–22;q23): Common Properties of Dysregulated Ras Pathway Signaling and Genomic Progression Characterize De Novo and Therapy-Related Cases. *American Journal of Clinical Pathology.* 2010;133(5):686-93.
77. Emerenciano M, Barbosa TdC, de Almeida Lopes B, Meyer C, Marschalek R, and Pombo-de-Oliveira MS. Subclonality and prenatal origin of RAS mutations in KMT2A (MLL)-rearranged infant acute lymphoblastic leukaemia. *British Journal of Haematology.* 2015;170(2):268-71.
78. Lavallée V-P, Baccelli I, Krosl J, Wilhelm B, Barabé F, Gendron P, et al. The transcriptomic landscape and directed chemical interrogation of MLL-rearranged acute myeloid leukemias. *Nature Genetics.* 2015;47(9):1030-7.
79. Kerstjens M, Driessen EMC, Willekes M, Pinhanços SS, Schneider P, Pieters R, et al. MEK inhibition is a promising therapeutic strategy for MLL-rearranged infant acute lymphoblastic leukemia patients carrying RAS mutations. *Oncotarget.* 2017;8(9):14835-46.
80. Hyrenius-Wittsten A, Pilheden M, Sturesson H, Hansson J, Walsh MP, Song G, et al. De novo activating mutations drive clonal evolution and enhance clonal fitness in KMT2A-rearranged leukemia. *Nature Communications.* 2018;9(1):1770.
81. Trentin L, Bresolin S, Giarin E, Bardini M, Serafin V, Accordi B, et al. Deciphering KRAS and NRAS mutated clone dynamics in MLL-AF4 paediatric leukaemia by ultra deep sequencing analysis. *Scientific reports.* 2016;6:34449-.
82. Kampen KR, ter Elst A, Mahmud H, Scherpen FJG, Diks SH, Peppelenbosch MP, et al. Insights in dynamic kinome reprogramming as a consequence of MEK inhibition in MLL-rearranged AML. *Leukemia.* 2014;28(3):589-99.
83. Janardhan HP, Milstone ZJ, Shin M, Lawson ND, Keaney JF, Jr., and Trivedi CM. Hdac3 regulates lymphovenous and lymphatic valve formation. *J Clin Invest.* 2017;127(11):4193-206.
84. Fernando TR, Contreras JR, Zampini M, Rodriguez-Malave NI, Alberti MO, Anguiano J, et al. The lncRNA CASC15 regulates SOX4 expression in RUNX1-rearranged acute leukemia. *Mol Cancer.* 2017;16(1):126.
85. O'Connell RM, Balazs AB, Rao DS, Kivork C, Yang L, and Baltimore D. Lentiviral Vector Delivery of Human Interleukin-7 (hIL-7) to Human Immune System (HIS) Mice Expands T Lymphocyte Populations. *PLOS ONE.* 2010;5(8):e12009.
86. Rao DS, O'Connell RM, Chaudhuri AA, Garcia-Flores Y, Geiger TL, and Baltimore D. MicroRNA-34a Perturbs B Lymphocyte Development by Repressing the Forkhead Box Transcription Factor Foxp1. *Immunity.* 2010;33(1):48-59.
87. Croker BA, Metcalf D, Robb L, Wei W, Mifsud S, DiRago L, et al. SOCS3 Is a Critical Physiological Negative Regulator of G-CSF Signaling and Emergency Granulopoiesis. *Immunity.* 2004;20(2):153-65.
88. de Boer J, Williams A, Skavdis G, Harker N, Coles M, Tolaini M, et al. Transgenic mice with hematopoietic and lymphoid specific expression of Cre. *European Journal of Immunology.* 2003;33(2):314-25.
89. Georgiades P, Ogilvy S, Duval H, Licence DR, Charnock‐Jones DS, Smith SK, et al. vavCre Transgenic mice: A tool for mutagenesis in hematopoietic and endothelial lineages. *genesis.* 2002;34(4):251-6.

90. Heffner CS, Herbert Pratt C, Babiuk RP, Sharma Y, Rockwood SF, Donahue LR, et al. Supporting conditional mouse mutagenesis with a comprehensive cre characterization resource. *Nature Communications.* 2012;3(1):1218.
91. Joseph C, Quach Julie M, Walkley Carl R, Lane Steven W, Lo Celso C, and Purton Louise E. Deciphering Hematopoietic Stem Cells in Their Niches: A Critical Appraisal of Genetic Models, Lineage Tracing, and Imaging Strategies. *Cell Stem Cell.* 2013;13(5):520-33.
92. Contreras JR, Palanichamy JK, Tran TM, Fernando TR, Rodriguez-Malave NI, Goswami N, et al. MicroRNA-146a modulates B-cell oncogenesis by regulating Egr1. *Oncotarget.* 2015;6(13):11023-37.
93. Heinz S, Benner C, Spann N, Bertolino E, Lin YC, Laslo P, et al. Simple combinations of lineage-determining transcription factors prime cis-regulatory elements required for macrophage and B cell identities. *Molecular cell.* 2010;38(4):576-89.
94. Quinlan AR, and Hall IM. BEDTools: a flexible suite of utilities for comparing genomic features. *Bioinformatics (Oxford, England).* 2010;26(6):841-2.
95. Mootha VK, Lindgren CM, Eriksson K-F, Subramanian A, Sihag S, Lehar J, et al. PGC-1α-responsive genes involved in oxidative phosphorylation are coordinately downregulated in human diabetes. *Nature Genetics.* 2003;34(3):267-73.
96. Subramanian A, Tamayo P, Mootha VK, Mukherjee S, Ebert BL, Gillette MA, et al. Gene set enrichment analysis: A knowledge-based approach for interpreting genome-wide expression profiles. *Proceedings of the National Academy of Sciences.* 2005;102(43):15545.
97. Xiao Y, Hsiao T-H, Suresh U, Chen H-IH, Wu X, Wolf SE, et al. A novel significance score for gene selection and ranking. *Bioinformatics (Oxford, England).* 2014;30(6):801-7.

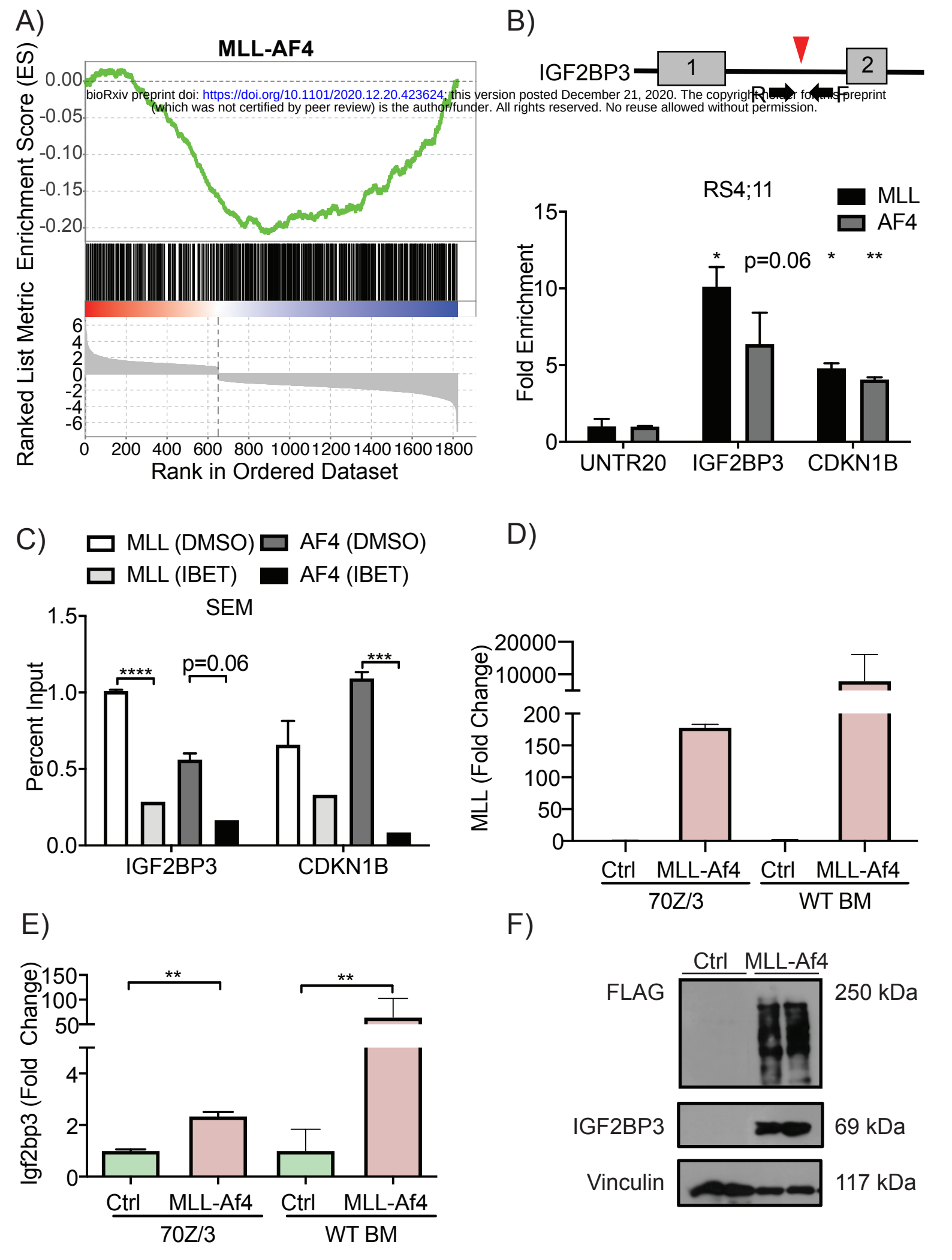

Figure 1

Figure 1: MLL-AF4 transcriptionally induces IGF2BP3.
A) GSEA of differentially expressed genes from IGF2BP3 depleted RS4;11 cells shows significant negative enrichment with MLL-AF4 ChIP targets (nominal P value: 0.001, FDR: 0.001, Normalized ES: -1.54)).
B) Schematic of MLL-AF4 binding site in intron 1 of IGF2BP3 (top). ChIP-qPCR shows fold enrichment for IGF2BP3 and CDKN1B with MLL and AF4 IP in RS4;11. Normalized to UNTR20, an untranscribed region (t-test; *P < 0.05, **P < 0.01).
C) Percent input from ChIP-qPCR of SEM cells show reduced binding of MLL-AF4 to IGF2BP3 with treatment of IBET151 (t-test; *** P < 0.001, ****P < 0.0001).
D) Expression of MLL through RT-qPCR of 70Z/3 transduced with either control (Ctrl) or MLL-Af4 vector selected with G418 and MLL expression at the RNA level in the BM of WT recipients transplanted with Ctrl or MLL-Af4 HSPCs.
E) Induction of Igf2bp3 at the RNA level in selected 70Z/3 with MLL-Af4 and in the BM of WT recipients transplanted with Ctrl or MLL-Af4 HSPCs (bottom) (t-test; **P < 0.01) .
F) Induction of Igf2bp3 at the protein level in BM from mice transplanted with MLL-Af4 transduced WT donor HSPCs.

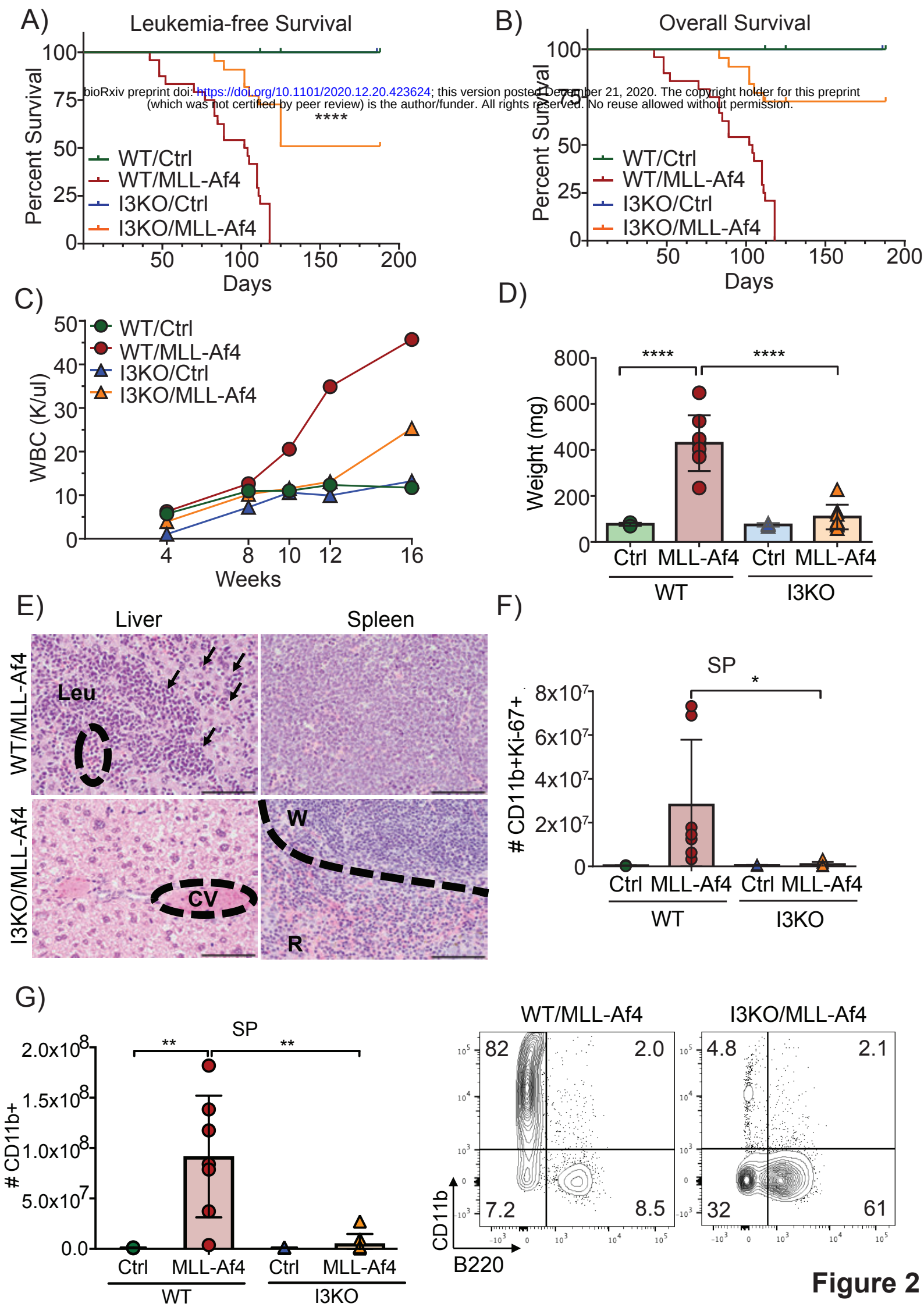

Figure 2

Figure 2: *Igf2bp3* deletion delays leukemogenesis and reduces disease severity.
A) Leukemia-free survival of mice transplanted with control (Ctrl) or MLL-Af4 transduced HSPCs from WT or Igf2bp3 KO mice (Kaplan-Meier method with Log-rank test; ****P < 0.0001).
B) Overall survival of mice transplanted with Ctrl or MLL-Af4 transduced HSPCs from WT or I3KO mice (n=12 WT/Ctrl, n=24 WT/MLL-Af4, n=7 I3KO/Ctrl, n=22 I3KO/MLL-Af4; Kaplan-Meier method with Log-rank test; ****P < 0.0001).
C) Time course of WBC in the PB of mice transplanted with Ctrl or MLL-Af4 transduced HSPCs from WT or I3KO mice (Data represented as means of three experiments; n=4 Ctrl, n=8 MLL-Af4 per experiment).
D) Spleen weights of mice transplanted with Ctrl or MLL-Af4 transduced HSPCs from WT or I3KO mice at 14 weeks (n= 4 Ctrl, n=8 MLL-Af4; one-way ANOVA followed by Bonferroni's multiple comparisons test; ****P < 0.0001).
E) H&E staining of liver and spleen of mice transplanted with mice transplanted with MLL-Af4 transduced HSPCs from WT or I3KO mice. Scale bar:100 microns; CV=Central vein; W=White pulp; R=Red pulp; Leu= Leukemia; arrows showing infiltration.
F) Quantitation of CD11b+Ki67+ cells in the spleen at 14 weeks post-transplantation (n= 4 Ctrl, n=8 MLL-Af4; one-way ANOVA followed by Bonferroni's multiple comparisons test; *P < 0.05).
G) (Left) Number of CD11b+ in the SP of recipient mice that received Ctrl or MLL-Af4 transduced HSPCs from WT or I3KO mice (one-way ANOVA followed by Bonferroni's multiple comparisons test; **P < 0.01). (Right) Corresponding representative FACS plots showing CD11b+ and B220+ cells in the SP.

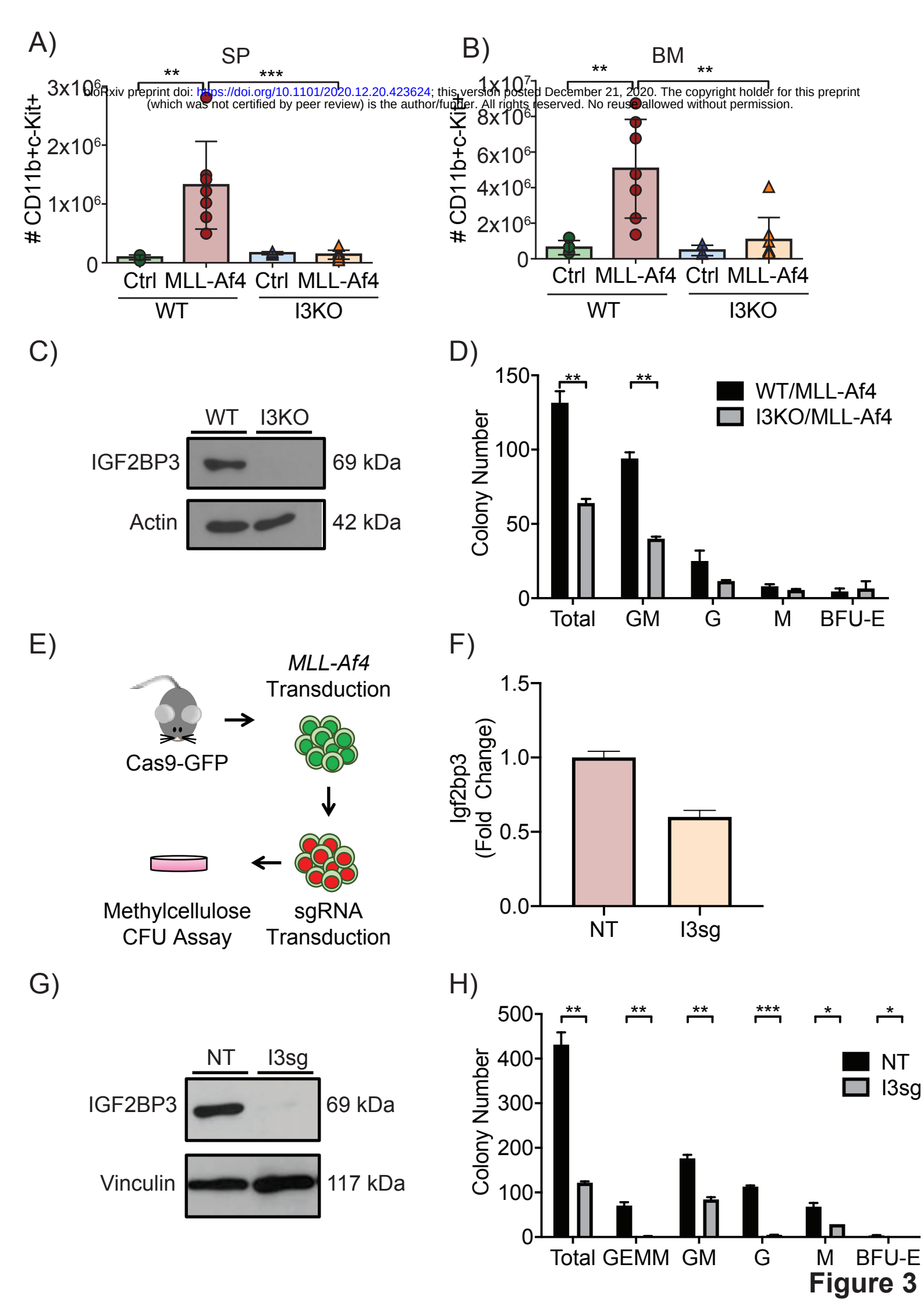

Figure 3

Figure 3: *Igf2bp3* is required for LIC function in endpoint colony formation assays.

A) Quantification of CD11b+c-Kit+ cells in the spleen of recipient mice at 14 weeks post-transplantation (n= 4 Ctrl, n=8 MLL-Af4; one-way ANOVA followed by Bonferroni's multiple comparisons test; **P < 0.01).

B) Quantitation of CD11b+c-Kit+ cells in the BM 14 weeks post-transplantation (n= 4 Ctrl, n=8 MLL-Af4; one-way ANOVA followed by Bonferroni's multiple comparisons test; **P < 0.01, ***P < 0.001).

C) Expression of IGF2BP3 of in WT/MLL-Af4 and I3KO/MLL-Af4 immortalized Lin- cells at the protein level.

D) Colony formation assay of WT/MLL-Af4 and I3KO/MLL-Af4 immortalized Lin- cells (t-test; **P < 0.01).

E) Schematic of collection of Cas9-GFP MLL-Af4 Lin- cells and CRISPR-Cas9 mediated deletion of *Igf2bp3*.

F) Expression of Igf2bp3 in Cas9-GFP MLL-Af4 Lin- cells in non-targeting (NT) and Igf2bp3 deleted (I3sg) cells by RT-qPCR.

G) Expression of IGF2BP3 in NT and I3sg Cas9-GFP MLL-Af4 Lin- cells at the protein level.

H) Colony formation assay of NT and I3sg deleted Cas9-GFP MLL-Af4 Lin- cells (t-test; *P < 0.05, **P < 0.01, ***P <0.001).

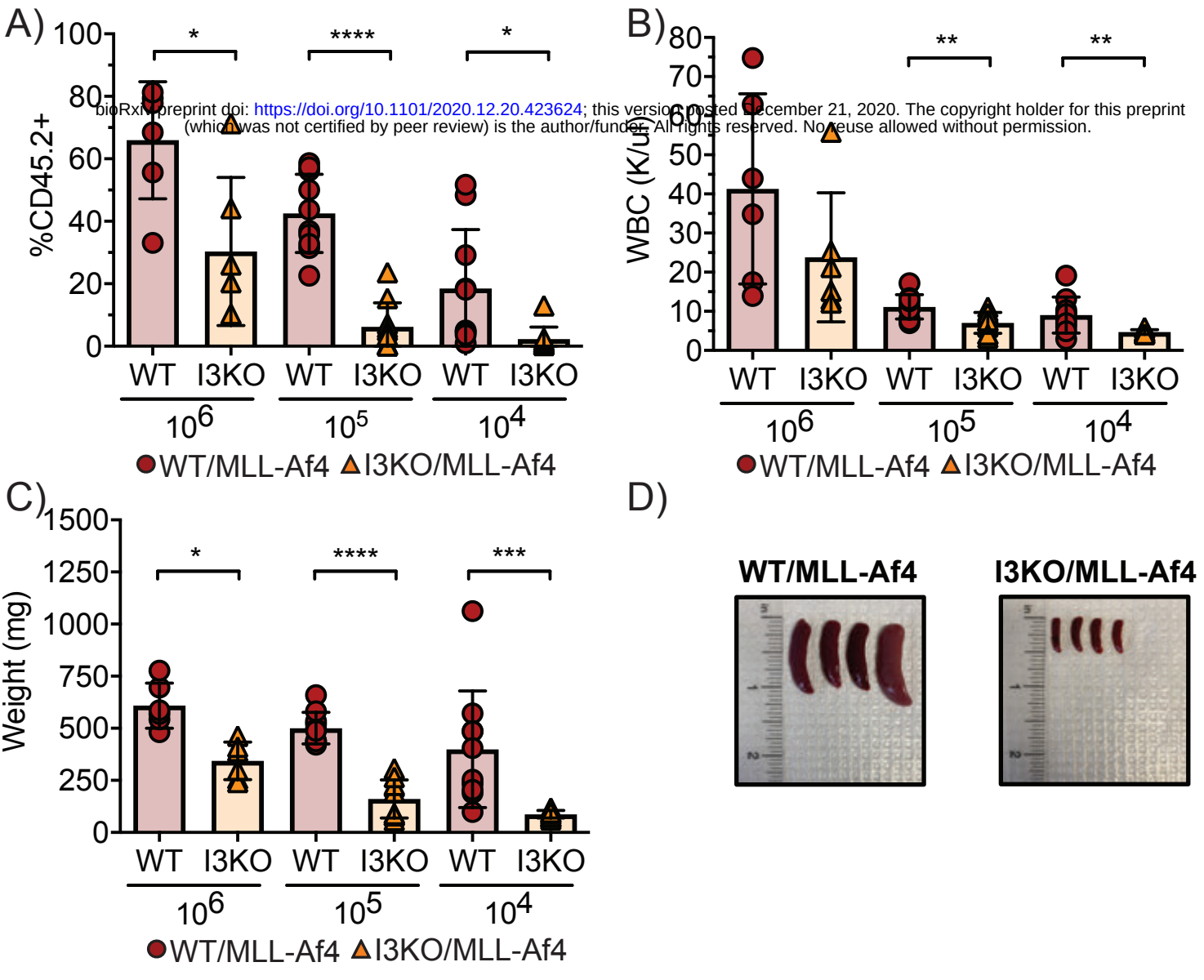

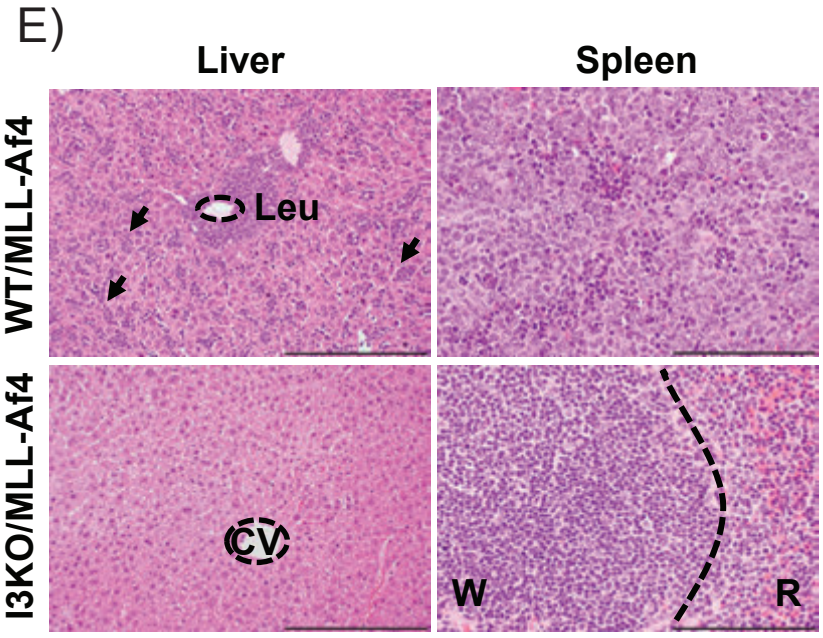

Figure 4

Figure 4: *Igf2bp3* deletion is necessary for MLL-Af4 leukemia-initiating cells to reconstitute mice *in vivo*.

A) Percentage of CD45.2+ in the peripheral blood of secondary transplanted mice from leukemic WT/MLL-Af4 or I3KO/MLL-Af4 donor mice at 10^6, 10^5, and 10^4 BM cells at 4 weeks post-transplantation (n= 6 10^6, n=10 10^5, n=10 10^4; t-test; *P < 0.05, ***P < 0.001, ****P < 0.0001).

B) WBC from PB of secondary transplanted mice from WT/MLL-Af4 or I3KO/MLL-Af4 BM 3-4 weeks post-transplant (n= 6 10^6, n=10 10^5, n=10 10^4; t-test; **P < 0.01).

C) Splenic weights of secondary transplanted mice at 4-5 weeks (n= 6 10^6, n=10 10^5, n=10 10^4; t-test; *P < 0.05, ***P < 0.001, ****P < 0.0001).

D) Images of splenic tumors in secondary mice transplanted with 10,000 BM cells from WT/MLL-Af4 mice (left) or I3KO/MLL-Af4 mice (right).

E) H&E staining of liver and spleen of secondary transplant recipients that received 10^5 cells. Scale bar: liver, 200 microns; spleen, 100 microns; CV=Central vein; W=White pulp; R=Red pulp; Leu= Leukemia; arrows showing infiltration.

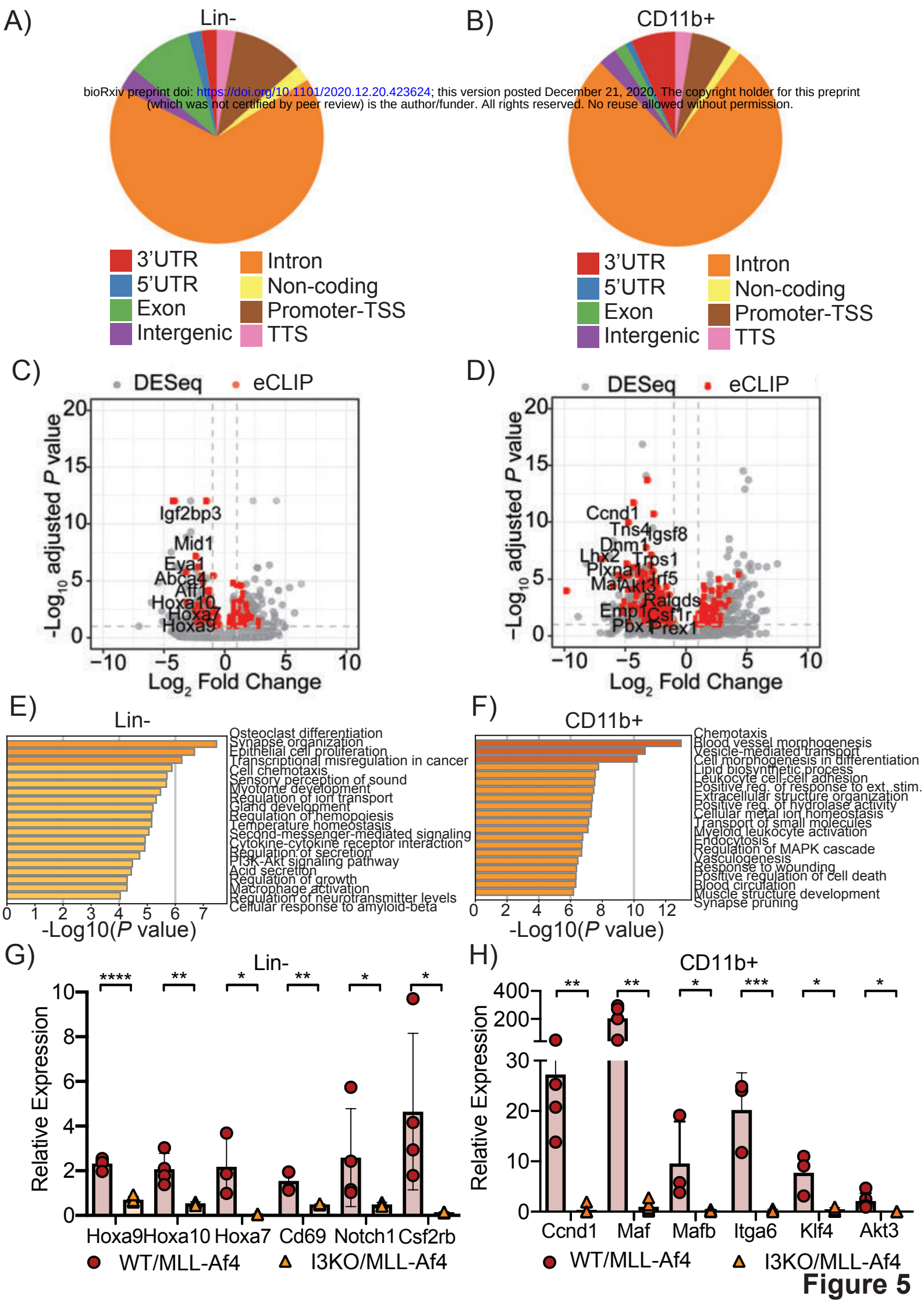

Figure 5

Figure 5: IGF2BP3 enhances MLL-Af4 mediated leukemogenesis through targeting transcripts within leukemogenic and Ras signaling pathways.

A) Genomic locations of IGF2BP3 eCLIP peaks in WT/MLL-Af4 Lin- cells

B) Genomic locations of IGF2BP3 eCLIP peaks in WT/MLL-Af4 CD11b+ cells.

C) Volcano plot of differentially expressed genes determined using DESeq analysis on RNA-seq samples from WT/MLL-Af4 or I3KO/MLL-Af4 Lin- cells. Dotted lines represent 1.0-fold–change in expression (vertical lines) and adjusted $P < 0.1$ cutoff (horizontal line). IGF2BP3 eCLIP-seq targets are highlighted in red.

D) Volcano plot of differentially expressed transcripts determined using DESeq analysis on RNA-seq samples from WT/MLL-Af4 or I3KO/MLL-Af4 CD11b+ cells. Dotted lines represent 1.0-fold–change in expression (vertical lines) and adjusted $P < 0.1$ cutoff (horizontal line). IGF2BP3 eCLIP-seq targets are highlighted in red.

E) GO Biological Processes and KEGG Pathway enrichment determined utilizing the Metascape enrichment analysis webtool on MLL-Af4 Lin- IGF2BP3 DESeq dataset with an adjusted $P < 0.05$ cutoff.

F) GO Biological Processes and KEGG Pathway enrichment determined utilizing the Metascape enrichment analysis webtool on MLL-Af4 CD11b+ IGF2BP3 DESeq dataset with an adjusted $P < 0.05$ cutoff. Bar graphs are ranked by P value and overlap of terms within gene list.

G) Expression of leukemogenic target genes in WT/MLL-Af4 and I3KO/MLL-Af4 Lin- cells by RT-qPCR (n= 4; t-test; *P < 0.05, **P < 0.01, ****P < 0.0001).

H) Expression of Ras signaling pathway genes in WT/MLL-Af4 and I3KO/MLL-Af4 CD11b+ cells by RT-qPCR (n=4; t-test; *P < 0.05, **P < 0.01, ***P < 0.001).

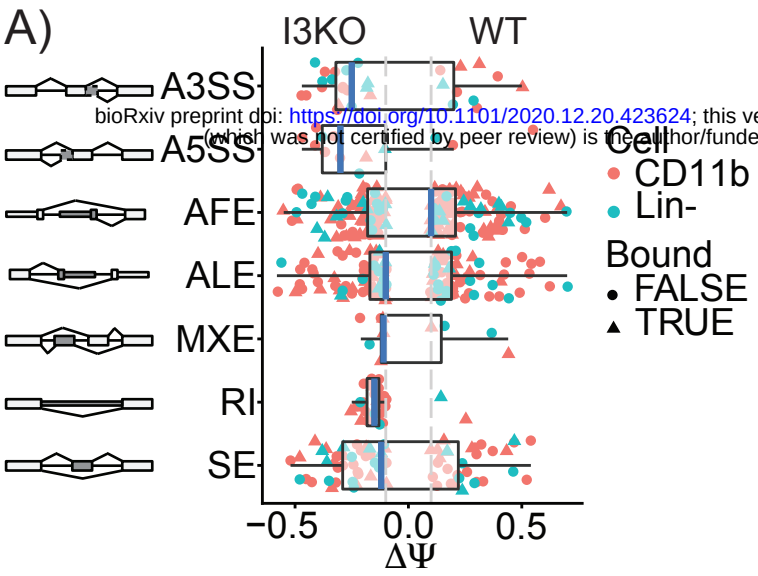

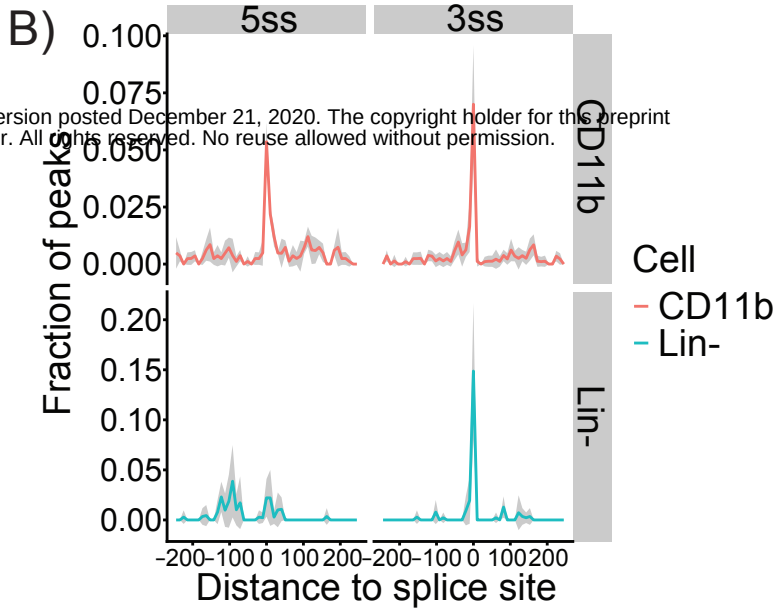

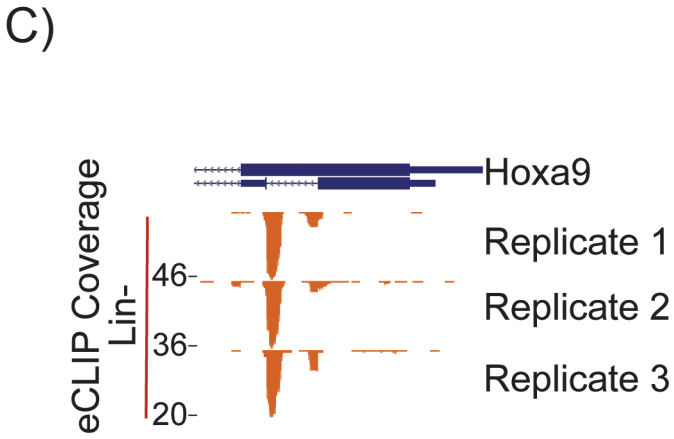

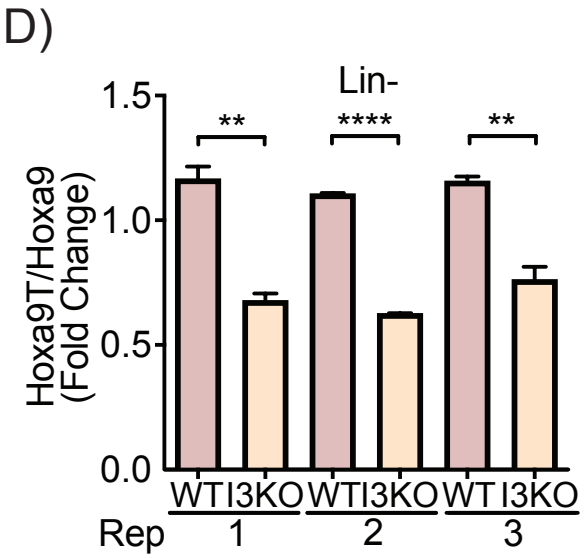

Figure 6

Figure 6: eCLIP analysis reveals IGF2BP3 function in regulating alternative pre-mRNA splicing.

A) Distribution of types of alternative splicing patterns for WT/MLL-Af4 or I3KO/MLL-Af4 Lin- and CD11b+ cells using MISO analysis. Delta psi values plotted indicate difference in isoforms.(A3SS, Alternative 3' splice sites; A5SS, Alternative 5' splice sites; AFE, Alternative first exons; ALE, Alternative last exons; MXE, Mutually exclusive exons; RI, Retained introns; SE, Skipped exons; Bound, IGF2BP3 eCLIP target).

B) Histogram showing normalized IGF2BP3 eCLIP peak counts and distance from IGF2BP3 eCLIP peak of 5' (5ss) and 3' (3ss) splice sites in WT/MLL-Af4 CD11b+ (top) cells and Lin- cells (bottom).

C) UCSC Genome Browser snapshots of the Hoxa9 loci. Each panel shows the exon-intron structure of the gene and unique read coverage from 3 eCLIP biological replicates from WT/MLL-Af4 Lin- cells. The maximum number of reads at each position is indicated to the left of each histogram.

D) Ratio of Hoxa9T/Hoxa9 isoforms in WT/MLL-Af4 and I3KO/MLL-Af4 Lin- cells by RT-qPCR (t-test; **P < 0.01, ****P < 0.0001).